CHAPTER 4

RESULTS AND DISCUSSION

4.1 Preliminary Tests on Silicon-Based Channels

We first observe the water wetting process in silicon-based channels with hydrophobic and hydrophilic surfaces, respectively. For hydrophobic surface, the silicon channel structure is treated with *Teflon*® solution; while for hydrophilic surface, treatment with O_2 plasma is adopted. The contact angles of water on the two surfaces are shown in Fig. 4-1.

4.1.1 Wetting Process in Hydrophobic Channels

The *Teflon*® coated chip is covered with a 3mm thick PMMA plate and sealed with silica glue. Two soft tubes are connected to two holes on the PMMA plate, to provide water and air, respectively, as shown in Fig. 4-2. The water is pumped at 0.2 *ml/min* and the air is pumped at 80 *ml/min*. The setting values are based on the assumption that DMFC operates at 100 mA/cm^2. For water, 0.2 *ml/min* is about five times than theoretical generation rate; while for air, 80 *ml/min* is about λ=4. During the first 15 seconds, water spreads out and fills the inlet zone without entering the channel section (see Fig. 4-2 (a)~(b)). This is because there exists a repulsive force in the hydrophobic channels. Subsequently, water enters the channel section forced by convective flow (Fig. 4-2 (c)). Water in channels near to the air inlet can be removed successful under forced convection. This is because the channel surface is hydrophobic, and the

flow resistance is therefore lower. In other channels far from the air inlet, water is trapped (Fig. 4-2 (d)). Hence, from this observation, we can know that water can be removed under medium flow rate with hydrophobic surface, but may suffered from partial flooded problem, especially in the low flow rate section.

We attempted to photograph the shape of water film through the PMMA plate, as shown in shown in Fig. 4-3. The shape appears slightly concave while a convex shape is expected for a hydrophobic surface. This should be owing to the slightly hydrophilic property of the top PMMA plate.

4.1.2 Wetting Process in Hydrophilic Channels

In this test, the O_2 plasma treated chip is covered with a glass plate, and water is provided by syringe pump with fixed flow rate (0.2 *ml/min*). Air flow is not provided and only capillary attraction is involved. The test begins without initial water film, as shown in Fig. 4-4(a). While water is dropped on the channel inlets, it is sucked into channels rapidly and then enters the buffer zone. The buffer zone is like a temporary reservoir that helps pump out the water film on the channel walls until it is filled with water. The recycling channels will then absorb the excessive water to maintain the pumping ability of the buffer zone.

In Fig. 4-4(b), the test is started with initial water film. In the parallel channels, the water transport speed is similar with the case with a initially-dry surface. Then, water enters the recycling channels rapidly without being delayed in the buffer zone as in the above case. This is because while hydrophilic surface is wetted, water can be more easily

transported with the presence of a thin film on the surface.

In Fig. 4-5, we further observe the water transport process with micrographs, with an amplification factor of ~100X. First, water is absorbed by the gap between the glass cover and channel ribs (Fig. 4-5 (1)~(2)). While water fills some of the channels (Fig. 4-5 (3)), it will overflow into the adjacent channels and forms convex shape by the adhesive force of water on glass (Fig. 4-5 (4)~(5)). Then, water is sucked into this channel from the inlet section. Since the capillary force of channel is larger than the adhesive force of water on glass, liquid film with convex shape therefore transforms into concave shape (Fig. 4-5 (6)~(7)). Finally, corner flow can be seen in the channels (Fig. 4-5 (8)).

From the above experiments and descriptions, it can be seen that a flow field with hydrophilic surface can provide a favorable recycling ability compared with hydrophobic one.

4.2 Assembly of Single DMFC

4.2.1 Integration of DMFC

In section 4.1, we have preliminarily demonstrated the feasibility of our proposed flow field. In order to observe the *in-situ* water formation and transport phenomena, we further fabricate a through-channel silicon flow field covered with a glass plate.

For the gas outlet section at the cathode side, a Teflon-treated carbon paper is adopted and covered on the buffer zone to achieve gas exhausting. The coating process has been introduced in Ch. 3. Fig. 4-6 shows the SEM images of carbon paper and the contact angles of water

on the carbon paper before and after the *Teflon*® treatment. After teflonization, the porosity of carbon paper clearly decreases and the contact angle of water increases by about seventeen degrees.

The completed single DMFC are shown in Fig. 4-7. For the operating conditions of DMFC, flow rates of fluids at anode and cathode have large effect on cell performance. Over-high flow rate may cause serious fuel crossover and waste too much auxiliary power, on the contrary, over-low flow rate may suffer from clogged problem of CO_2 bubbles and liquid water. As mentioned by Cowart [29], anode flow stream from 10 to 100 times the base stoichiometric ratio is often used to maximize the cell performance. From his suggestion, very high stoichiometries (>20) is needed; for cathode side, low air stoichiometries (λ<5) will result in poor cell performance because of saturated air exit streams. According to this reference, different flow rates are tested to make a comparison with above version for this study (Table 4-1).

4.2.2 In-situ Visualization of Cathode side for Micro DMFC

In our earlier tests, we inserted a layer of stainless steel mesh between the flow field and the carbon cloth as the electric conductor. This layer covers the front two-third area from the inlet section. The test conditions are shown in Table 4-2. For a DMFC, the power output would reach a steady state after fuel be supplied for about 15~20 minutes. The formation of water droplets in the cathode side during the start-up time is shown in Fig. 4-8. In the beginning, some fog can be seen on the surface of glass but disappear with the temperature rise of glass. Then, water vapor gradually condenses into small droplets, which aggregate on the

glass. The following data were measured after the DMFC operated for about 20 minutes.

At high current load operation, some interesting phenomena are observed (Fig. 4-9). For the inlet section, there is no liquid water in the channels (air flow rate at 80 *ml/min*). Liquid water droplets and slugs appear in the middle section of the flow channels, where flooding can be seen. Interestingly, flooding becomes alleviated in the rear portion of the flow channels where the stainless steel layer is not present, as shown by the smaller water droplets here. The different behaviors of water respectively associated with stainless steel mesh and carbon cloth can be observed. As the stainless steel mesh, is slightly hydrophilic, water tends to be trapped in the texture to result in water flooding. In contrast, the carbon cloth is hydrophobic and water forms a number of droplets on its surface. This is more clearly shown in Fig. 4-10, the added stainless steel mesh will form a gap (~100μm) between channel ribs and carbon cloth. This may affect the behavior of water transport.

Later on, the stainless steel mesh is replaced with a number of silver-coated wires. The water transport behavior is shown in Fig. 4-11. It is likely that water exists in the bottom corners as well as on the rib walls (the images are captured upward). Water films can be seen on both sides of the channels. Besides, water transport can also be observed by the slight regular motion of the films. If the air flow rate is suddenly increased, the water films clearly turn thinner but maintain their slight regular motion. This is an interesting and encouraging result. Fig. 4-12 compares the water film thickness at different air flow rates. At a high flow rate (80 *ml/min*), the film thickness is clearly thinner (each water

film reduces by ~40μm) than that at low flow rate (40 *ml/min*). At a flow rate as low as 10 *ml/min*, the water films on either side remain separated. All the channels with observation opening are found to be free from clogging. The capillary force on the hydrophilic surface is shown to successfully handle the water generation to result in continuous water films on the channel walls and a continuous flow in the bottom channel corners.

4.2.3 Performance testing of micro DMFC

Fig. 4-13 shows the flow field with gold-plated surface. Fig. 4-14 shows the polarization curve of two different hydrophilic surfaces: one is SiO_2 and the other is plated with Au. In the test of flow field with SiO_2 surface, its maximum current and power output are 67 mA at 0.016V, 6.528 mW at 0.272V, respectively. The possible reasons for the poor efficiency and the rapidly dropped current are the high electronic and ionic resistances in the materials.

For the Au-plated flow field, we attempt to make observation opening but failed due to the fracture during laser-cutting. It is the bottleneck of laser-cutting fabrication process, the crack of flow field easily happened in over-deep structure. Hence, the flow field without observation opening is then integrated into a single DMFC and its efficiency is tested under the same conditions as before. It can be seen that the efficiency of gold-plated flow field has improved conspicuously, says the maximum current and power output are respectively 308 mA at 0.016V and 36.816 mW at 0.208V, which the increase rates are about 4.6 and 5.6 times than flow field with SiO_2-induced surface.

From above test, there are two possible reasons for the efficiency improvement of DMFC. First, the conspicuous decrease of electronic resistance in the flow field material; second, the deeper channel depth (from 250μm to 400μm) makes a slower air flow and a larger air capacity. More oxygen can therefore get into catalyst layer per unit time.

Additionally, make a comparison between the multi-sectional design in this study and Yang et al. [23]. In their study, they concluded that the hydrophilic gas channel is the main mechanism for water removal, but if the liquid film became thicker, the gas channel might be blocked. On the contrary, there is no blocked problem in our testing result even with low air flow rate. This may attributed to the design of buffer zone and recycling channels, which make the end of parallel channels become more unhindered and form a workable loop.

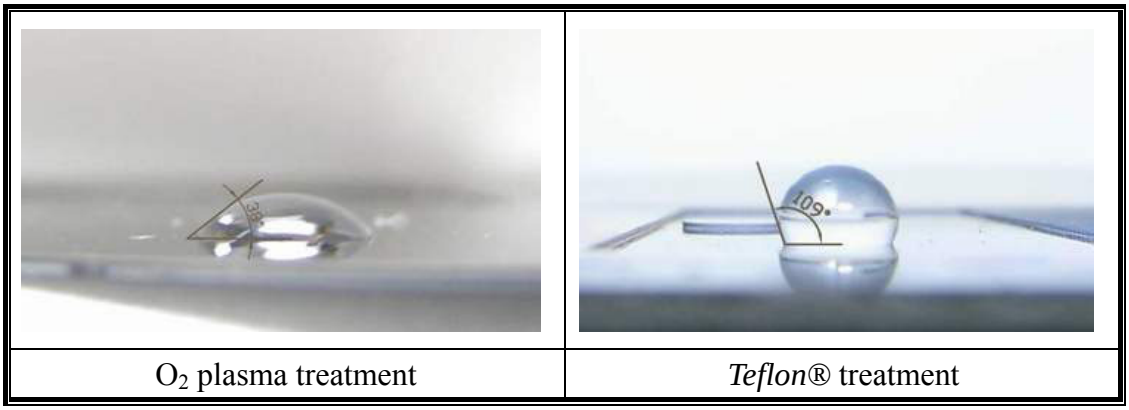

O_2 plasma treatment	*Teflon*® treatment

Fig. 4-1 Contact angle of water on hydrophilic/hydrophobic treatment surface

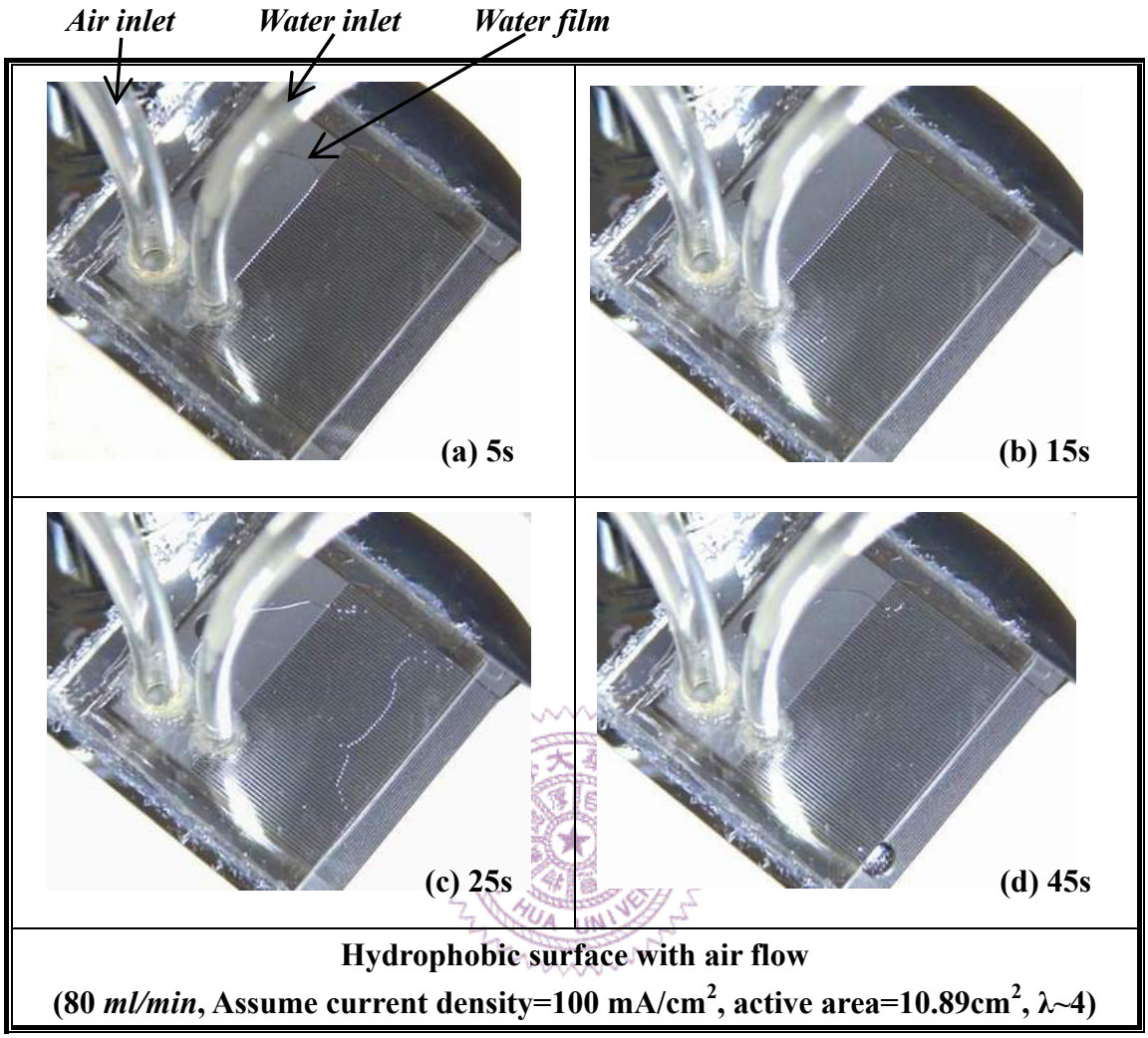

Fig. 4-2 Dynamic process of flow pattern for hydrophobic silicon chip

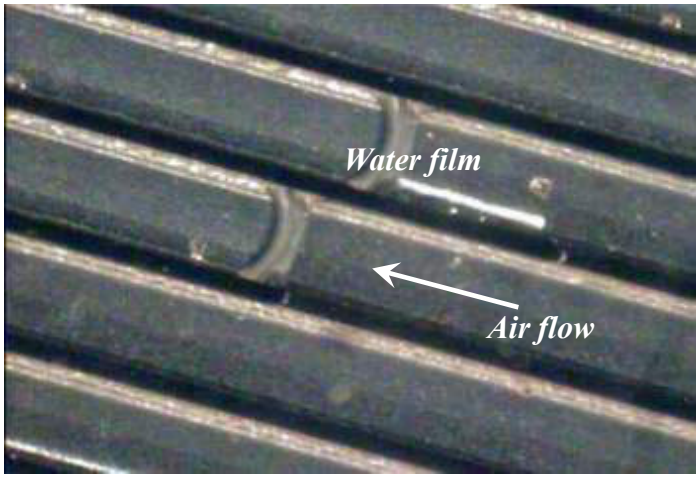

Fig. 4-3 Shape of liquid film for hydrophobic silicon chip

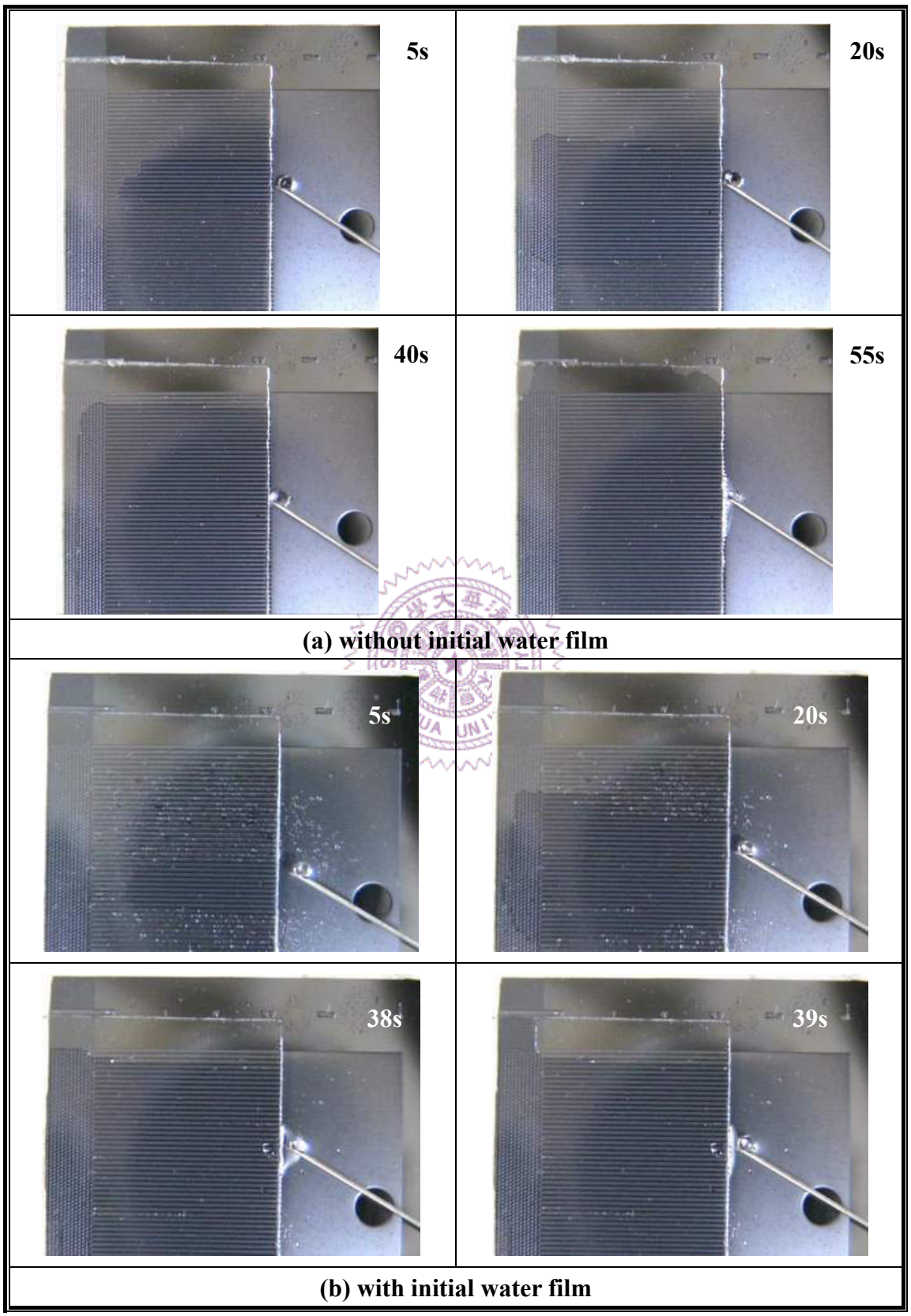

Fig. 4-4 Dynamic process of flow pattern for hydrophilic silicon chip

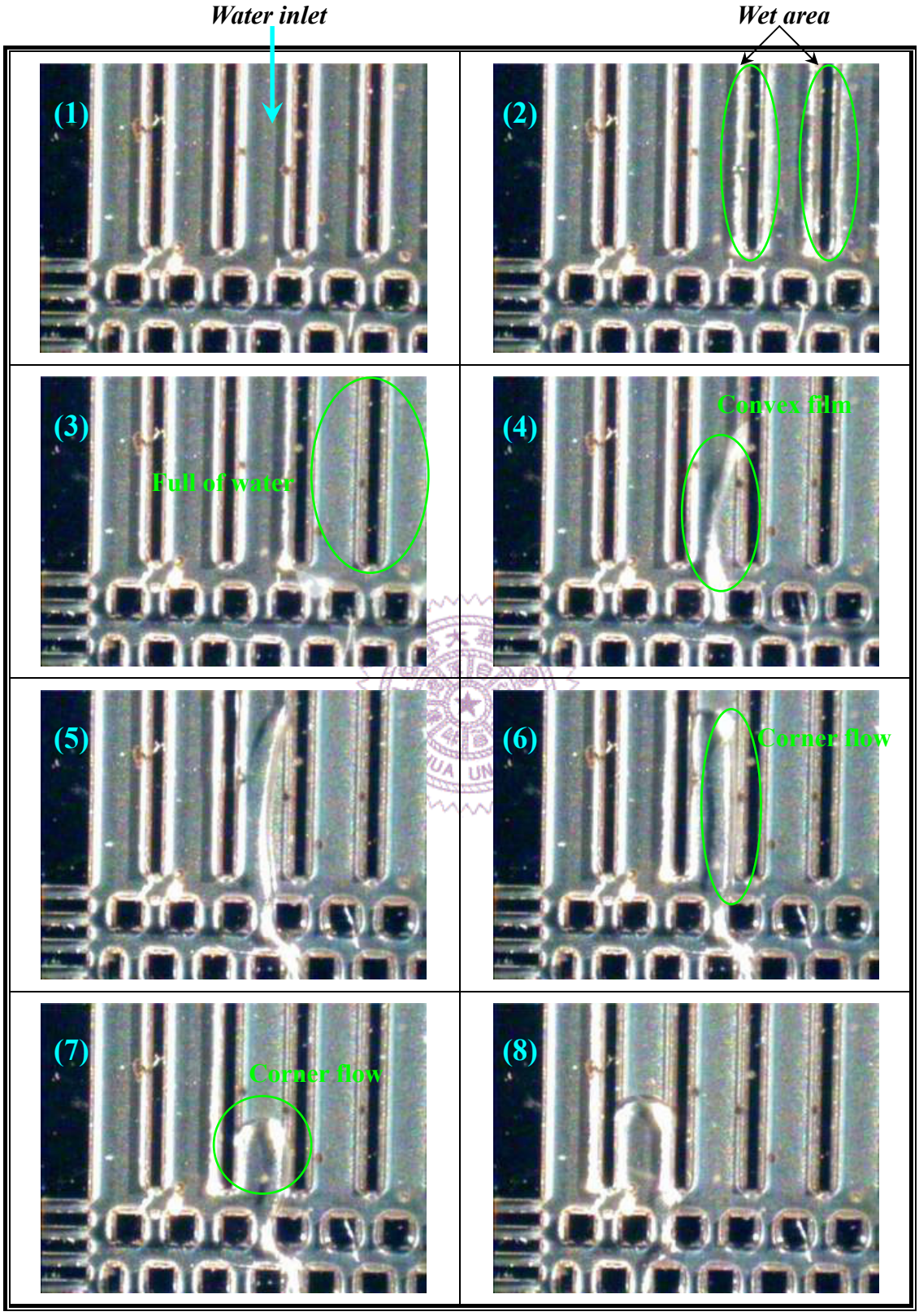

Fig. 4-5 Dynamic process of flow pattern for hydrophilic Si flow field

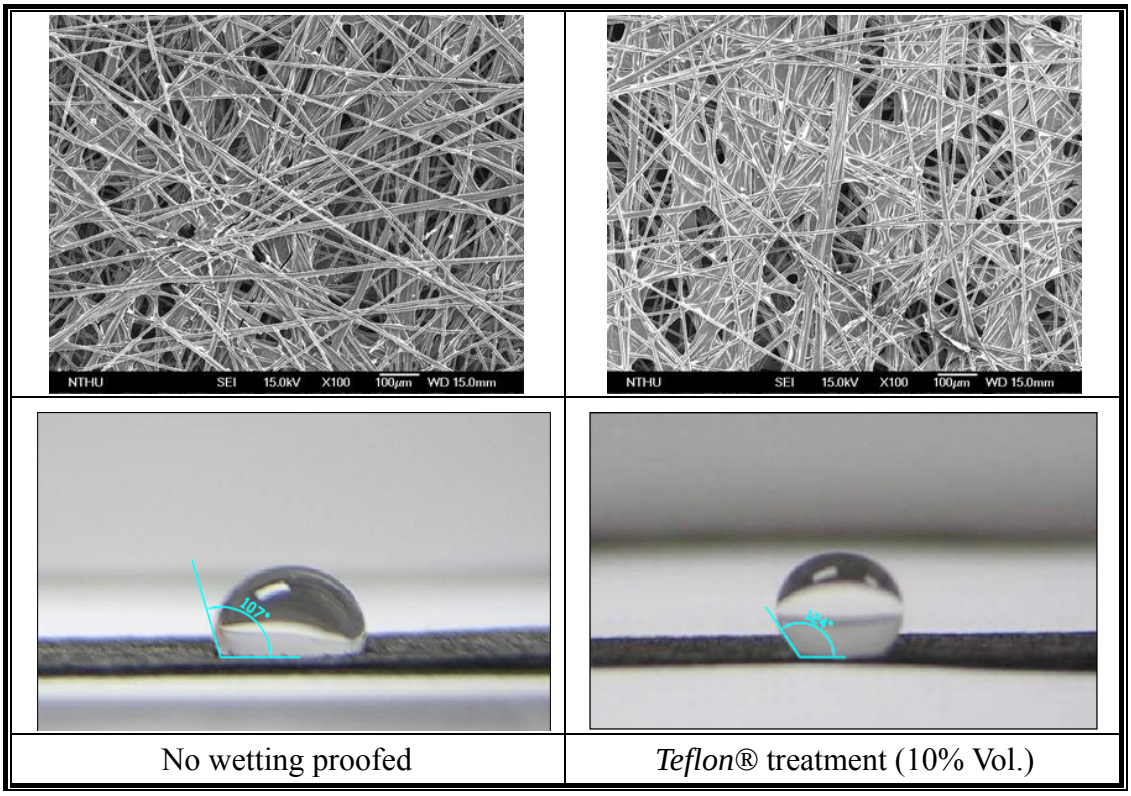

Fig. 4-6 SEM images and contact angles of water on carbon papers

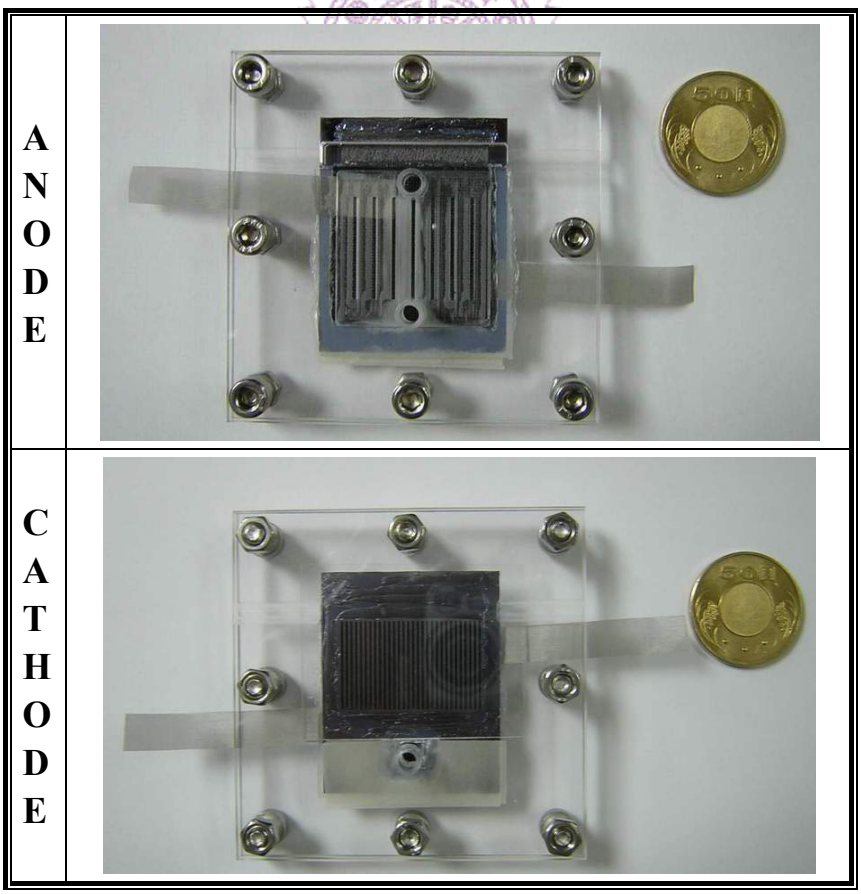

Fig. 4-7 Schematic of integrated single-DMFC

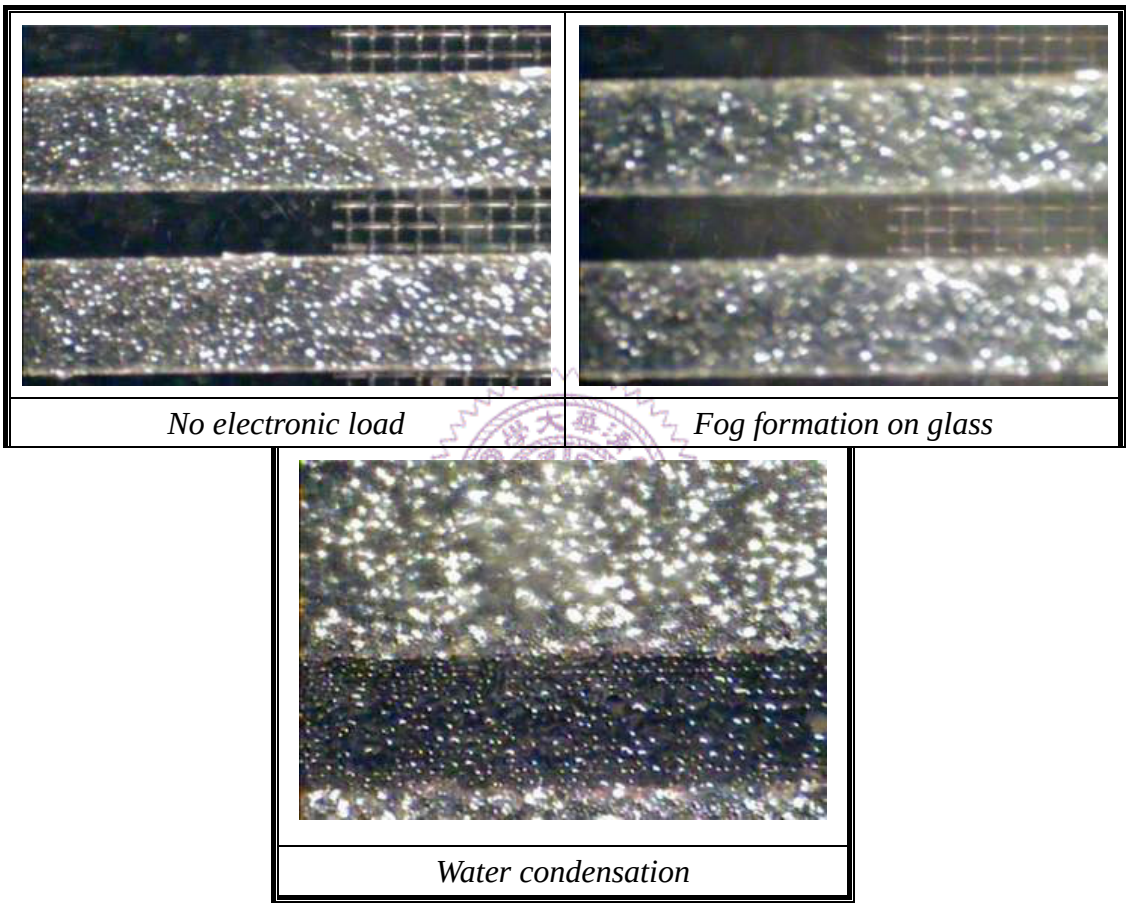

Fig. 4-8 Schematic of water droplets formation in the flow field

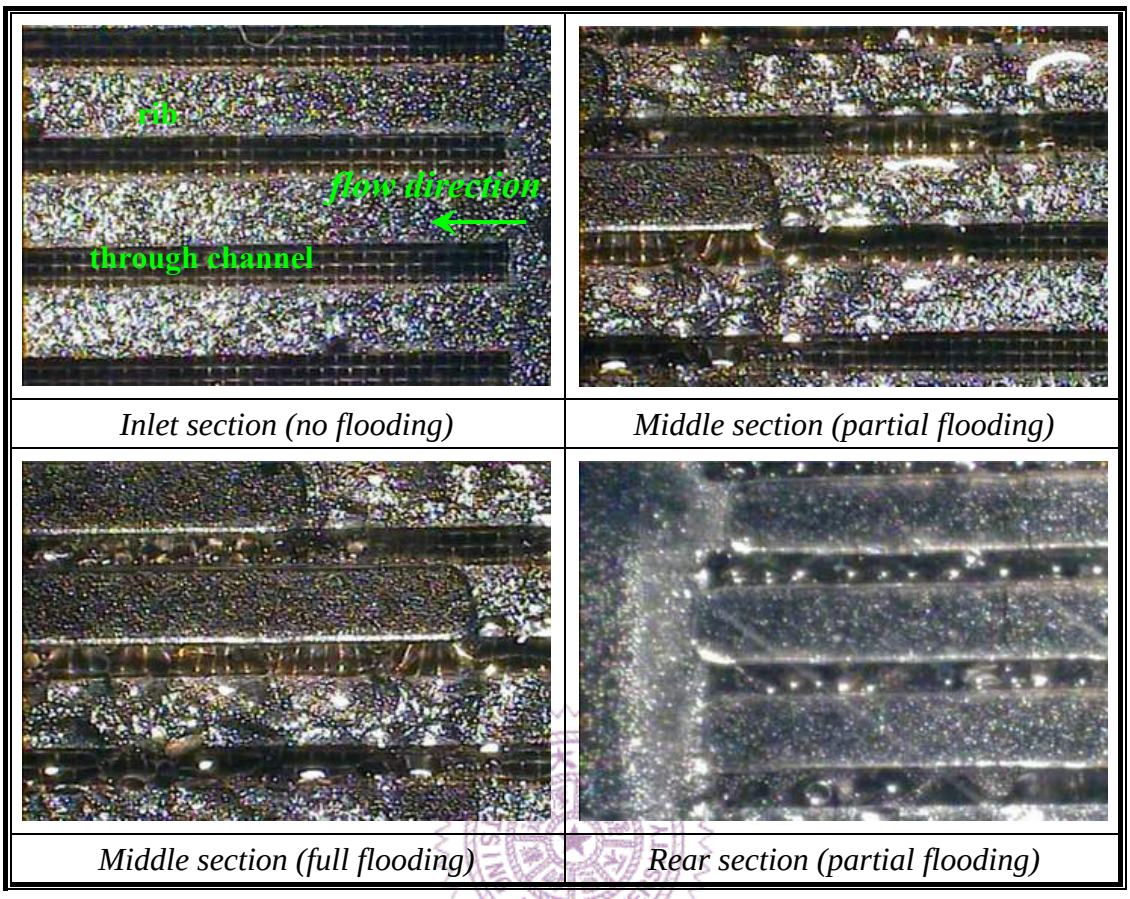

Fig. 4-9 Visualization of water distribution in the flow field

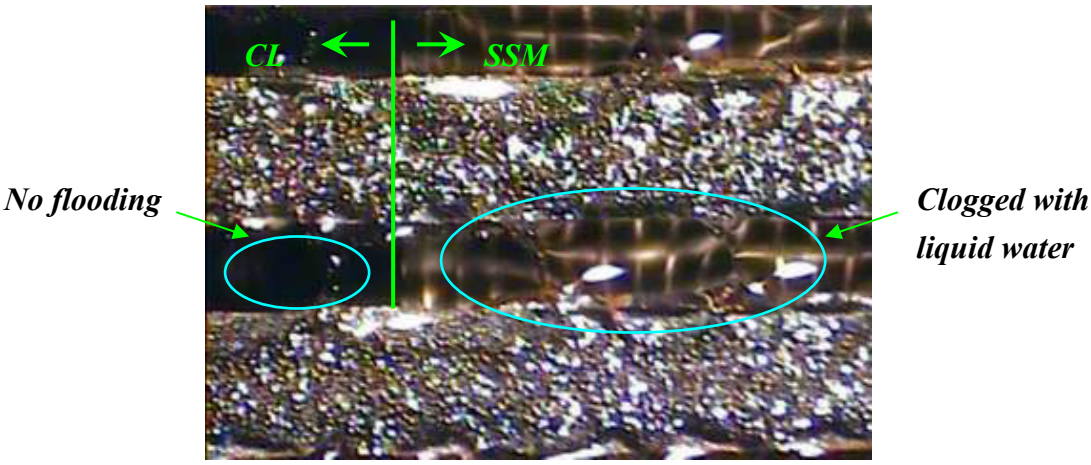

Fig. 4-10 Visualization of water droplets behavior on different surfaces (CL: carbon cloth; SSM: stainless steel mesh)

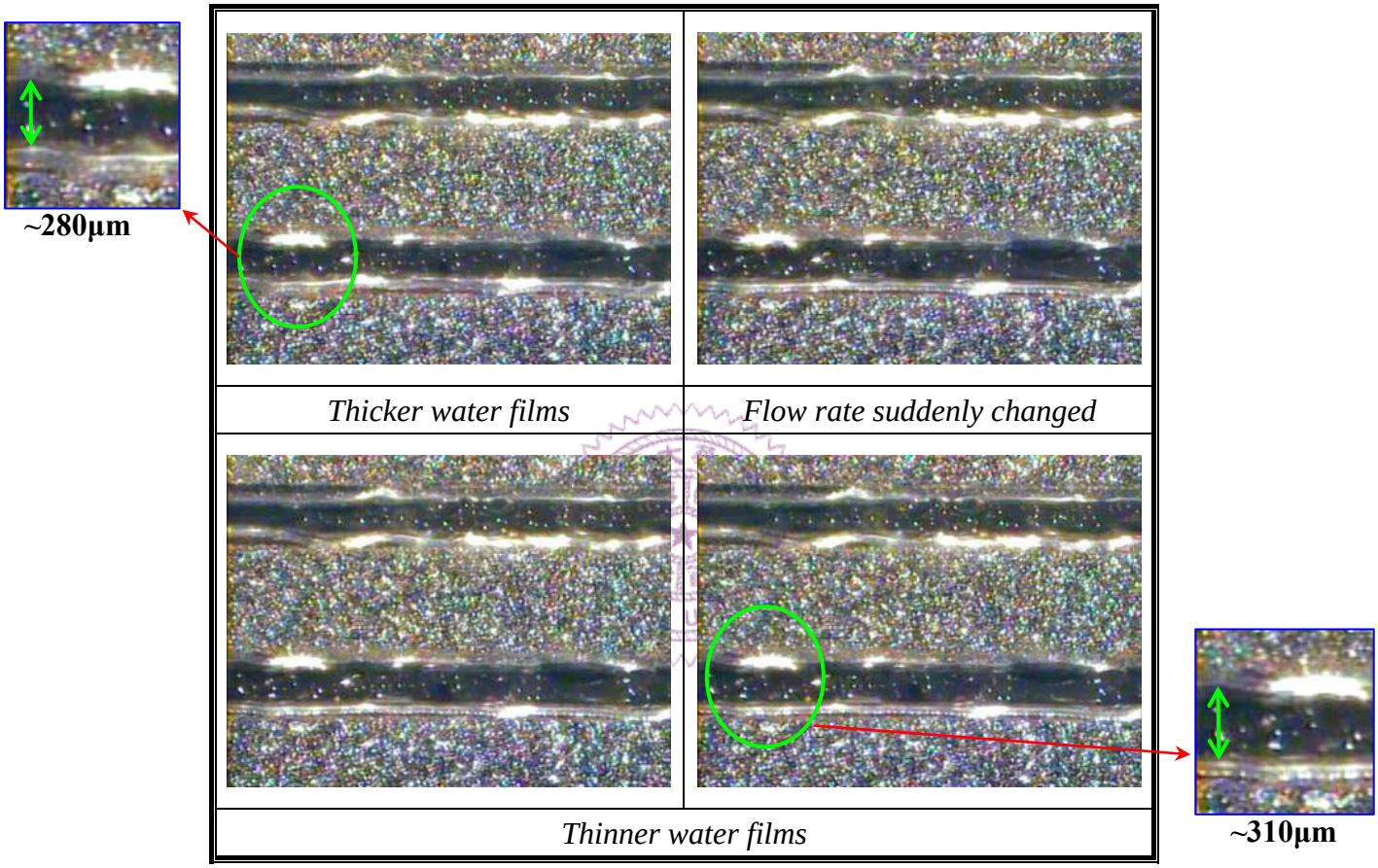

Fig. 4-11 Dynamic process of water film behavior

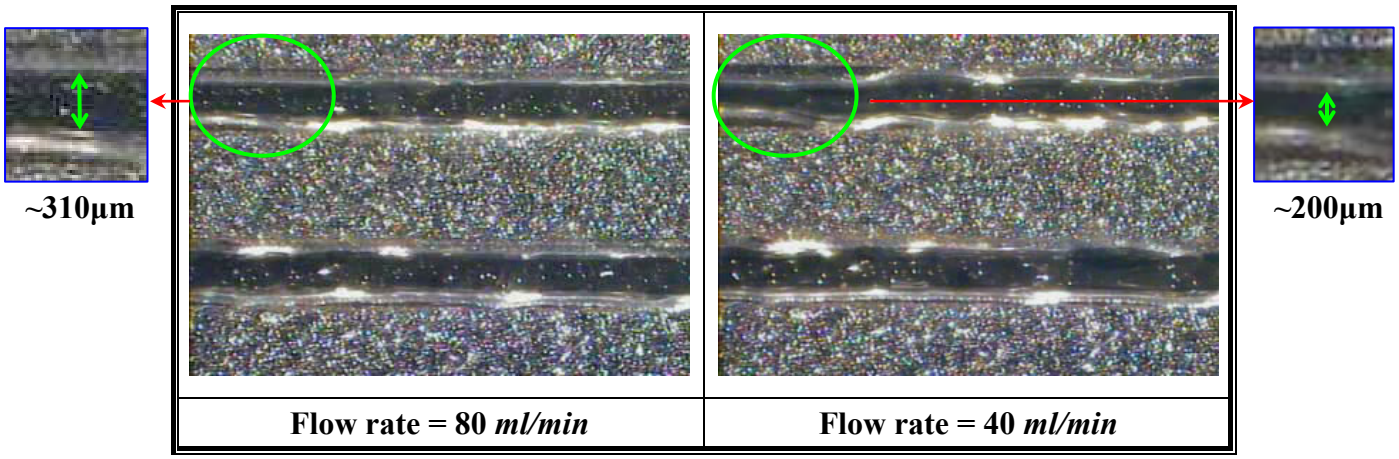

Fig. 4-12 Accumulative behavior of water films with different flow rates

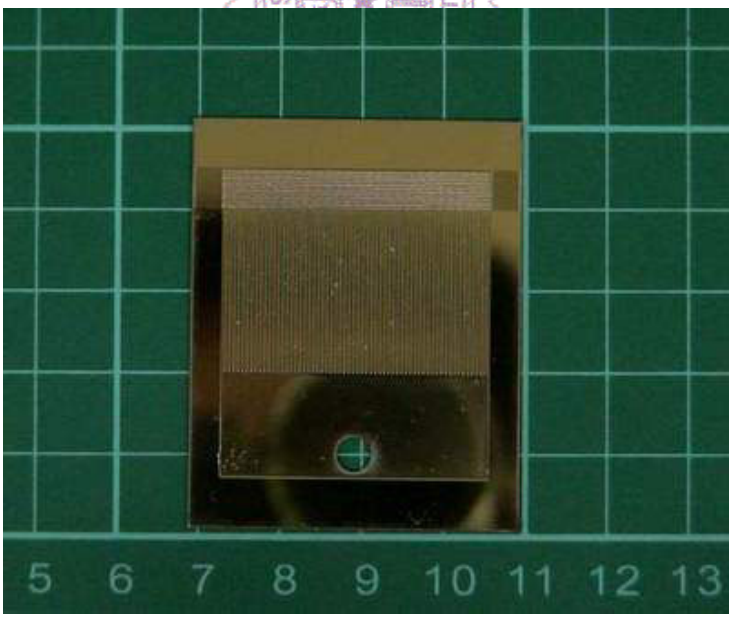

Fig. 4-13 Schematic of gold-plated multi-sectional flow field

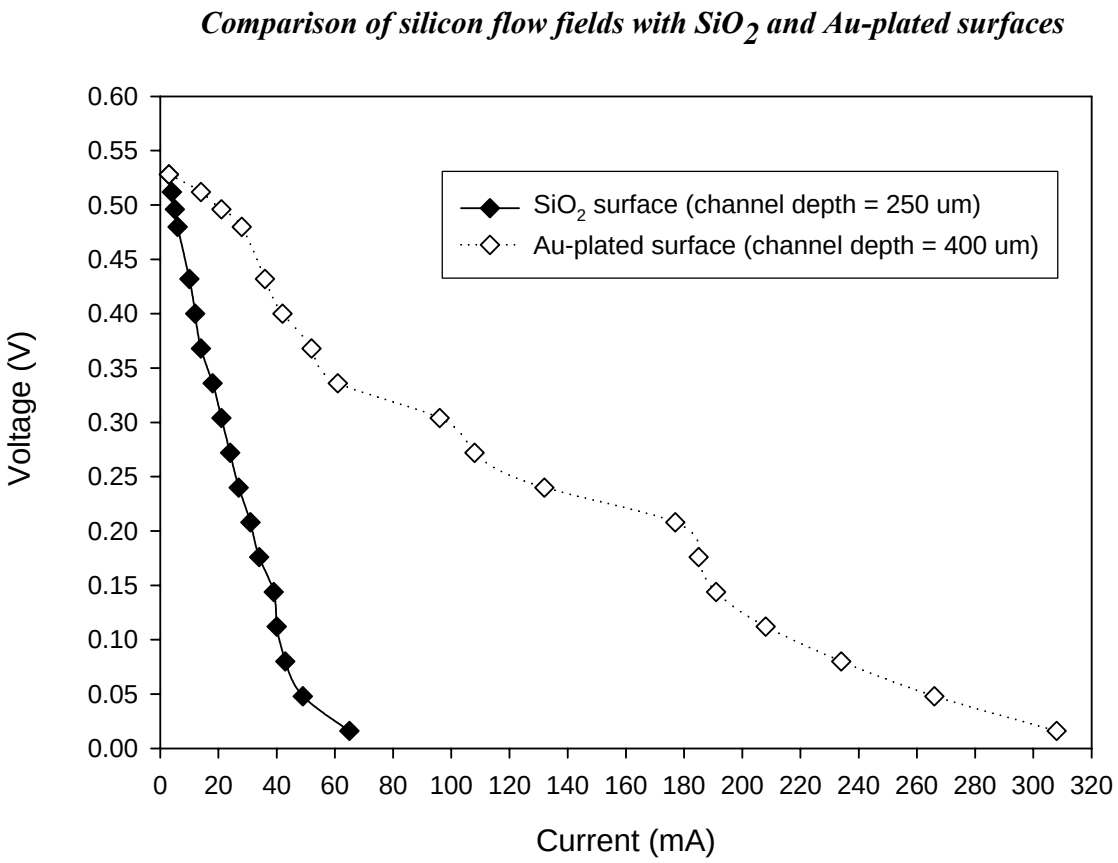

Fig. 4-14 Polarization curves of DMFC with SiO_2 and Au-plated flow fields

Table 4-1 Air and Methanol stoichimetric ratios for the DMFC

Active area = 10.89 cm^2, Current density = 100 mA/ cm^2 is assumed		
	Flow rate(ml/min)	***λ***
Anode (4M MeOH)	2	70
Cathode (Air)	20	1
	40	2
	80	4

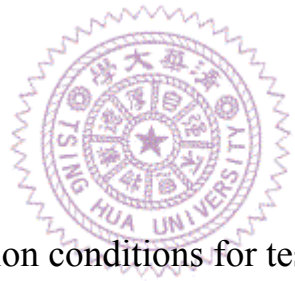

Table 4-2 Operation conditions for tested single DMFC

Anode	4M Methanol solution, flow rate = 2 *ml/min*
Cathode	Non-humidified air, 1atm, room temperature, flow rate 0 ~ 80 *ml/min*